ARMY RESEARCH LABORATORY

Etching Characteristics and Surface Analysis of Molecular Bean Epitaxy Grown p-type Aluminum Gallium Nitride With Boron Trichloride/Chlorine Gases in Inductively Coupled Plasma (ICP) Dry Etching

by Fred Semendy, Phillip Boyd, and Unchul Lee

ARL-TR-3370 **November 2004**

NOTICES

Disclaimers

The findings in this report are not to be construed as an official Department of the Army position unless so designated by other authorized documents.

Citation of manufacturer's or trade names does not constitute an official endorsement or approval of the use thereof.

Destroy this report when it is no longer needed. Do not return it to the originator.

Army Research Laboratory
Adelphi, MD 20783-1197

ARL-TR-3370 **November 2004**

Etching Characteristics and Surface Analysis of Molecular Bean Epitaxy Grown p-type Aluminum Gallium Nitride With Boron Trichloride/Chlorine Gases in Inductively Coupled Plasma (ICP) Dry Etching

Fred Semendy, Phillip Boyd, and Unchul Lee
Sensors and Electron Devices Directorate, ARL

REPORT DOCUMENTATION PAGE

Form Approved
OMB No. 0704-0188

1. REPORT DATE *(DD-MM-YYYY)*	2. REPORT TYPE	3. DATES COVERED (From - To)
November 2004	Final	

4. TITLE AND SUBTITLE
Etching Characteristics and Surface Analysis of Molecular Bean Epitaxy Grown p-type Aluminum Gallium Nitride With Boron Trichloride/Chorine Gases in Inductively Coupled Plasma (ICP) Dry Etching

5a. CONTRACT NUMBER

5b. GRANT NUMBER

5c. PROGRAM ELEMENT NUMBER

6. AUTHOR(S)
Fred Semendy, Phillip Boyd, and Unchul Lee

5d. PROJECT NUMBER

5e. TASK NUMBER

5f. WORK UNIT NUMBER

7. PERFORMING ORGANIZATION NAME(S) AND ADDRESS(ES)
U.S. Army Research Laboratory
ATTN: AMSRD-ARL-SE-EM
2800 Powder Mill Road
Adelphi, MD 20783-1197

8. PERFORMING ORGANIZATION REPORT NUMBER
ARL-TR-3370

9. SPONSORING/MONITORING AGENCY NAME(S) AND ADDRESS(ES)
U.S. Army Research Laboratory
2800 Powder Mill Road
Adelphi, MD 20783-1197

10. SPONSOR/MONITOR'S ACRONYM(S)

11. SPONSOR/MONITOR'S REPORT NUMBER(S)

12. DISTRIBUTION/AVAILABILITY STATEMENT
Approved for public release; distribution unlimited.

13. SUPPLEMENTARY NOTES

14. ABSTRACT

Dry etching of magnesium doped p-type aluminum gallium nitride grown by molecular beam epitaxy (MBE) has been carried for the first time by inductively coupled plasma (ICP) system via the boron trichloride/chlorine (BCl_3/Cl_2) gas system with variations in chuck power, ICP power, cholrine (Cl_2) ratio in Cl_2/BCl_3 and process pressure. Processed samples were cleaned by standard techniques, depths were measured, and etching rates and selectivity were calculated. Surface morphology of the etched samples was analyzed by atomic force microscopy (AFM) and scanning electrom microscopy (SEM). Etching rates were influenced by ICP power, and chuck power increased chlorine ratio in BCl_3/Cl_2 and process pressure. The increase in the etching rate is caused by an increased number of chloride radicals created by high inductive power and increased ion flux and thus, physical bombardment and chemical etching components are enhanced. In most cases, the selectivity with respect to the photo-resistance was higher than 1. AFM showed a smooth surface for the etched samples compared to the un-etched control sample. Roughness values increased initially, followed by a drop indicating the increased smoothness of the surface. Auger electron spectroscopic (AES) studies show that there is a reduction of intensity in the etched samples. Calculations indicated that the gallium/nitrogen decreased slightly in the etched sample, which indicated a very small percentage of nitrogen deficiency because of surface-induced damage by etching. This might give rise to changes in resistance and ohmic contact formation.

15. SUBJECT TERMS
ICP, etching, AlGaN, BCl_3/Cl_2

16. SECURITY CLASSIFICATION OF:			17. LIMITATION OF ABSTRACT	18. NUMBER OF PAGES	19a. NAME OF RESPONSIBLE PERSON
a. REPORT	b. ABSTRACT	c. THIS PAGE			Fred Semendy
Unclassified	Unclassified	Unclassified	UL	21	19b. TELEPHONE NUMBER (*Include area code*) 301-394-4627

Contents

List of Figures

1. Introduction

There is a tremendous push in technology to use III-nitrides for high temperature electronics and photonic devices. The ability to process gallium nitride (GaN) and related materials for electrical and optical device applications is highly important for the advancement of future high temperature and high power electronic and opto-electonic devices. Fabrication of a wide variety of GaN-based photonic and electronic devices depends on dry etching. Such devices include laser diodes (*1*), light-emitting diodes (LEDs) (*2*), hetero-junction bipolar transistors (*3,4,5*), p-type – intrinsic-n-type (p-i-n) photodiodes (*6,7,8*), and junction field effect transistors (*9*). Currently, aluminum gallium nitride (AlGaN) has become an important material for ultraviolet (UV) emitters and detectors, primarily because of the tunability of its band gap from that of GaN (3.4 eV) to that of aluminum nitride (AlN) (6.2eV) through variation of the AlN mole fraction (*10*). Deep UV LEDs with their potential applications in solid state lighting, biochemical detection, and high-density data storage have recently been a focus of intense research and development. In the fabrication of the III-nitride-based mesa structures, it is beneficial to etch through AlGaN alloys with a single etching recipe. Since III-nitride devices are based on hetero-structures with a variety of compositions, it is necessary to develop dry etching conditions that can effectively cover the entire composition range of $Al_xGa_{1-x}N$ alloys. Because of the relatively high bond energy (8.92eV/atom) of GaN, the threshold ion energy for the onset of dry etching is typically on the order of 25eV (*11*). Plasma-assisted dry processing techniques such as reactive ion etching (RIE), inductively coupled plasma etching (ICP), and electron cyclotron resonance (ECR) have shown the most promising results. Most opto-electronic devices require consistent, repeatable, anisotropic, high etching rates, and etching by the RIE method has been the method of choice. However, the wide band gap material-based devices require smooth surface morphology, low damage, and selective etching of one material over another. Since the plasma density in ICP etching is much higher, the results obtained with ICP etching are two or four orders of magnitude higher for the etching rates for the group-III nitrides as compared to RIE (*12,13,14*). Generally, the etching characteristics will be strongly affected by the choice of reactive gases, and the etching rates are often limited by the volatility of the III-nitride products. Halogen-based chemistries are preferred to etch gallium (Ga)- and aluminum (Al)-containing materials because of the high volatility of the etching products compared to fluorine-based products (*15*). Etching behavior of GaN, $Al_xGa_{1-x}N$, and AlN has been systematically studied in an ICP plasma etching with chlorine (Cl_2) and argon (Ar) as the reagents (*16*). Smith et al., found that the etching rates were strongly influenced by ICP and chuck powers but insensitive to pressure, flow rate, and gas compositions. Etching characteristics of $Al_xGa_{1-x}N$ grown by metal-organic-chemical-vapor deposition (MOCVD) were investigated in an ICP etching system that used a Cl_2/Ar gas mixture (*17*). It was found that the etching rate increased with ICP power and chuck power, whereas it decreased with an increase in the Al composition. Dry etching of

undoped n- and p-type GaN films has been performed in ICP system with a Cl_2/Ar gas mixture, and the authors have found similar etching behavior in all the GaN films (*18*). Dry etching with ICP was performed on n-type GaN with Cl_2/BCl_3 chemistry (*19*). In another study, it was found that the etching rates for n-type GaN samples for similar conditions were higher than the etching rate of p-type GaN (*20*). In general, etching rates of GaN are higher than AlGaN, regardless of plasma conditions. Al in AlGaN decreases the etching rates because of the higher bond strength between Al and N. The etching rate of AlGaN can be enhanced by the addition of BCl_3 to Cl_2 gas. However, little work has been done on the ICP etching of molecular beam epitaxy (MBE) grown p-type AlGaN films with Cl_2/BCl_3 chemistry. In this study, we report for the first time etching rates and selectivities of p-AlGaN as a function of BCl_3/Cl_2 ratio, various ICP and chuck power, and gas pressure with a Unaxis Versalock 700 (VLR) series modular cluster plasma ICP processing system. We report the etching rates during various conditions and the surface morphologies obtained with atomic force microscopy (AFM), scanning electron microscopy (SEM), and auger electron spectroscopic (AES).

2. Experiment

AlGaN layers were grown on c-plane, 2-inch sapphire substrates by MBE with RF atomic nitrogen plasma source (*21*). In this system, effusion cells provide flux of the group III element gallium and the p-type dopant magnesium. Typically, the RF source is operated at 400 W. For the material we used for the study (grown by SVT[1] Associates, Inc.), 200 nm of AlN buffer were grown on top of a c-plane sapphire, followed by a 0.4-µm thick undoped GaN layer and then a thick layer that was graded over 0.1-µm film. Finally, 1 µm AlGaN (20% Al, Mg-doped) was grown on top. The as-grown layer is measured to 2.5 by $10^{17}cm^{-3}$ at ambient temperature with mobility of 10 $cm^2cm^{-1}s^{-1}$, with indium/zinc (In/Zn) for electrical contacts. Before etching, samples were cut into 5- by 5-mm squares and cleaned with trichloro acetylene (TCA), acetone, iso propyl alcohol (IPA), and deionized water and then blow dried with nitrogen. Standard photolithographic techniques were used with AZ 5214 to create a 1.4-µm thick photoresistance mask (AZ5214) containing 7-µm stripes separated by 200 µm.

In this experiment, we used the VLR. It is a cluster-style plasma-processing system designed to service micro-fabrication requiring high performance, thin-film dry etching and or/deposition. The system contains a load module (LM), transport module (TM), and three process modules (PMs). Materials to be processed are mounted on a 4-inch sapphire or silicon wafer with cool grease for proper substrate cooling with a minute of heating at 50 ºC and transferred to a cassette and then introduced into the LM. In all experiments, the gas pressure was maintained at 5 mTorr, and the substrate and the electrode temperatures (T1 and T3) were usually kept at

[1]Name of company; not an acronym.

25 ºC. In this system, helium was used to produce a constant temperature for the various etching conditions. In all experiments, the gas flow rates were maintained at Cl_2 at 20 standard cubic centimeter (sccm) and BCl_3 at 15 sccm except when the Cl_2 ratio was varied in the Cl_2-BCl_3 gas combination.

We determined etching rates by the step heights measured with a KLA-Tencor[2] P 15 profilometer by measuring the feature depths before and after the removal of photoresistance. Anisotropy was determined by SEM. Surface roughness was examined by AFM before and after the etching of lapped samples via the tapping mode with calibrated silicon (Si) tip. Surface analysis was performed on selected samples by X-ray photoelectron spectroscopy (XPS) with the Physical Electronics PHI 5800 XPS System.

3. Results and Discussion

The effect of chuck power variation on the etching rates on p-AlGaN and the selectivity are plotted an figure 1(a) and (b). The chuck power is increased gradually in 100-watt steps, starting from 75 W and ending at 400 W with the ICP power maintained at 500 W. The etching rate increased from 1960 Å/min to 5003 Å/min at a maximum of 400 W. As can be seen from the graph, the etching rate increased monotonically as the chuck power increased, reached a maximum at around 300 W and remained almost the same around 400 W. When we look at the data, the etching rate was 4916 Å/min at 300 W and 5003 Å/min, showing a deceleration of etching rate. The initial increase in the etching rate can be explained as attributable to an increase in ion bombarding energy. The increase in etching rate can be attributed to an increasing sputter desorption of each product as well as more efficient breaking of the Ga-N bonds as the ion energy is increased. The selectivity is plotted against chuck power in figure 1(b). As the cathode power increases, the ion bombardment also increases, and as a result, the selectivity changes direction and decelerates and decreases with the increased sputter yielding of photoresistance. This etching rate is very similar to what others have obtained for AlGaN with Cl_2/Ar gas system. They obtained an etching rate of 3020 A/min for a bias voltage of –250 V.

[2]Name of a company; not an acronym.

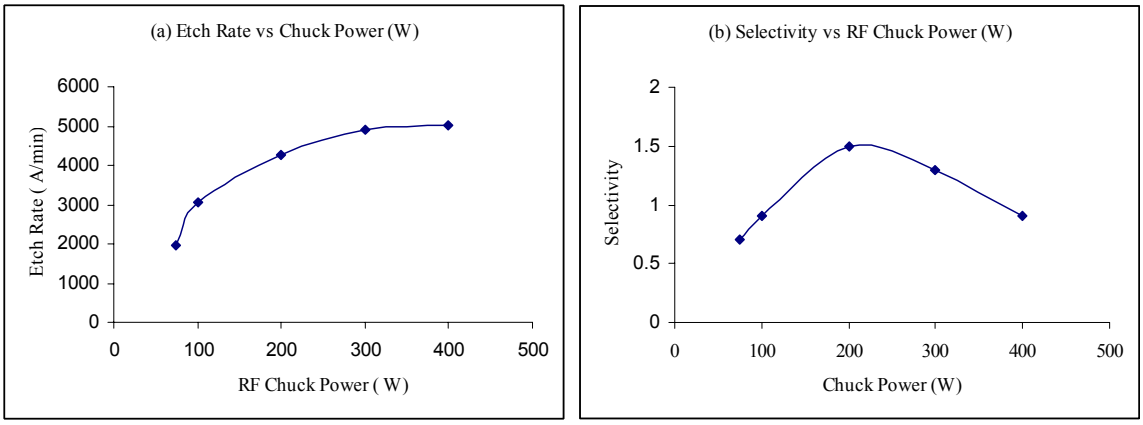

Figure 1. (a) p-AlGaN etching rates with different RF cathode power; (b) selectivity of p-AlGaN over photoresistance versus cathode power. (The process conditions are 500 W of ICP power, 20 sccm Cl_2, and 15 sccm BCl_3.)

In the next set of experiments, we examined the etching rate of p-AlGaN with the changes in the ICP power. In these experiments, the gas pressure was maintained at 5 mTorr, the substrate and the electrode temperatures (T1 and T3) were usually kept at 25 ºC, the gas flow rates were maintained at Cl_2 at 20 sccm, and BCl_3 at 15 sccm, and the radio frequency (RF) chuck power was kept constant at 300 W and the ICP power was varied. The results of the etching rate changes and the selectivity changes with ICP power variations are plotted in figure 2 (a) and (b), respectively.

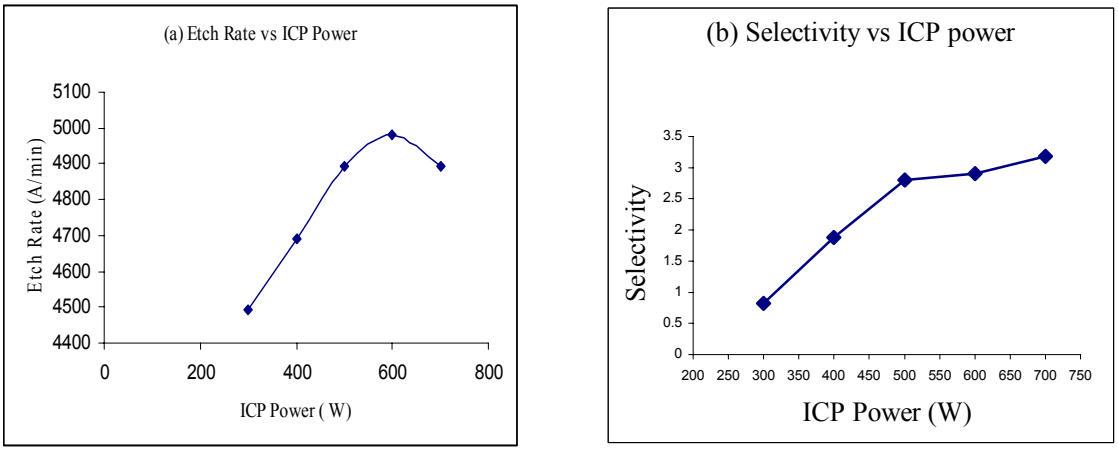

Figure 2. (a) Variations of p-AlGaN etching rates with different ICP power; (b) selectivity of p-AlGaN material over photoresistance versus ICP power. (The process conditions are 300 W of chuck power, 20 sccm Cl_2, and 15 sccm BCl_3.)

As can be seen from the graph, the etching rates increased with increasing ICP power. The ICP power was changed from 300 W to 700 W with a step increase of 100 W. For 300 W, we obtained an average etching rate of 4493 Å/min and 4874 Å/min for 700 W ICP power. As the ICP power increased, the etching rate increased because of higher concentrations of reactive

species producing higher etching rates. Because of an increase in ion flux, the bonds are broken more and there is an increase of sputter desorption. At higher ICP power, the etching rate decreases. We have observed that the DC bias voltage decreased as the ICP power increased. Thus, at high ICP power, the bias voltage is smaller, which will produce low ion energy plasma that will make the etching rate decrease at higher ICP power. The lower etching rate can thus be attributed to sputter desorption of reactants from the surface before they have time to react. The selectivity is plotted in figure 2 (b). As the ICP power changes, we see a corresponding change in the selectivity and we observe the selectivity increasing because of the damage on the photresistance initially but less pronounced for additional ICP power.

Variation of Cl_2 concentration was done in the next set of experiments to obtain etching rates and selectivity with respect to the percentage of increased Cl_2 ratio in BCl_3/Cl_2. In figure 3 (a), p-AlGaN etching rates are shown as a function of Cl_2 percentage in BCl_3/Cl_2 gas mixture and in figure 3 (b) shows selectivity.

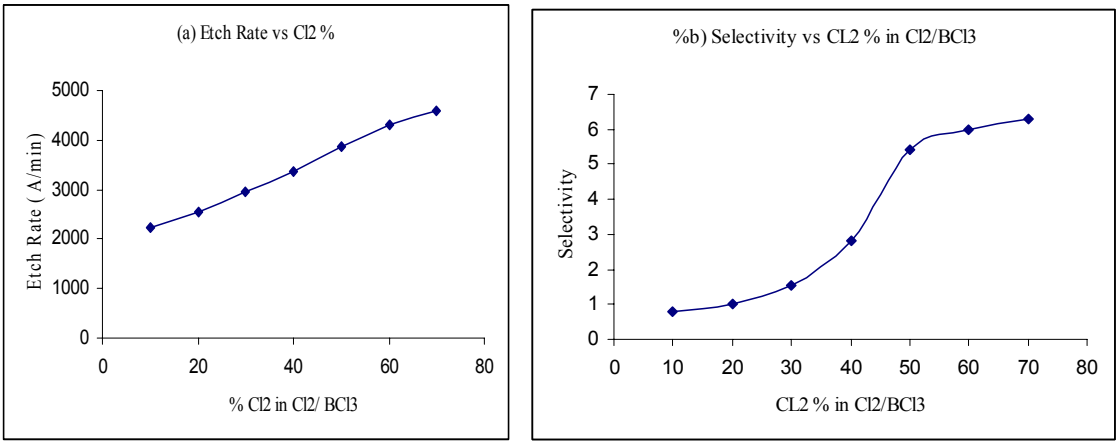

Figure 3. (a) Variations of etching rates for p-AlGaN for different %Cl_2 in BCl_3/Cl_2 ratio (the ICP power is 500 W and chuck power 200 W); (b) plot of selectivity as a function of Cl_2 percentage in BCl_3/Cl_2 gas mixture.

The increase in Cl_2 flow in the BCl_3/Cl_2 ratio increases the etching rate of p-AlGaN. In the experiment, the total gas feed rate is kept constant at 35 sccm and the ICP power at 500 W and the chuck power at 200 W and pressure at 5 mTorr. When the chlorine concentrations increase, more chlorine radicals are produced, which increases the etching rate.

The physical bombardment changes as the chlorine concentrations and the degree of dissociation change, which lead to the enhancement of chemical reaction. In the dissociation mechanism, one can get two Cl atoms from a single molecule of Cl_2 but only one atom of Cl for a single molecule of BCl_3. As a result of more Cl atoms from Cl_2, the etching rate increases. The Cl_2 was changed to 70% in the experiment. However, as can be seen in figure 3 (b), the selectivity over photoresistance increased slowly with increasing percentage of Cl_2 ratio and then jumped to a higher selectivity ratio, indicating damage of photoresistance because of increased availability of

chlorine radicals. In the next set of experiments, the chamber pressure was changed from 5 mTorr to 25 mTorr. The etching rates were measured and the selectivity calculated, and both are plotted in figure 4 (a) and (b). As can be seen from the graph, the etching rate clearly dropped after around 15 mTorr. This decrease in etching rates is because the mean free path that the ions have to travel is much shorter at higher pressure than at 15 mTorr. At higher pressure, kinetic energy is lower, creating more collisions between ions, causing the plasma to be much denser. The selectivity of p-AlGaN with respect to the photoresistance also shows a similar pattern because of lower plasma densities or polymer formation on the surface.

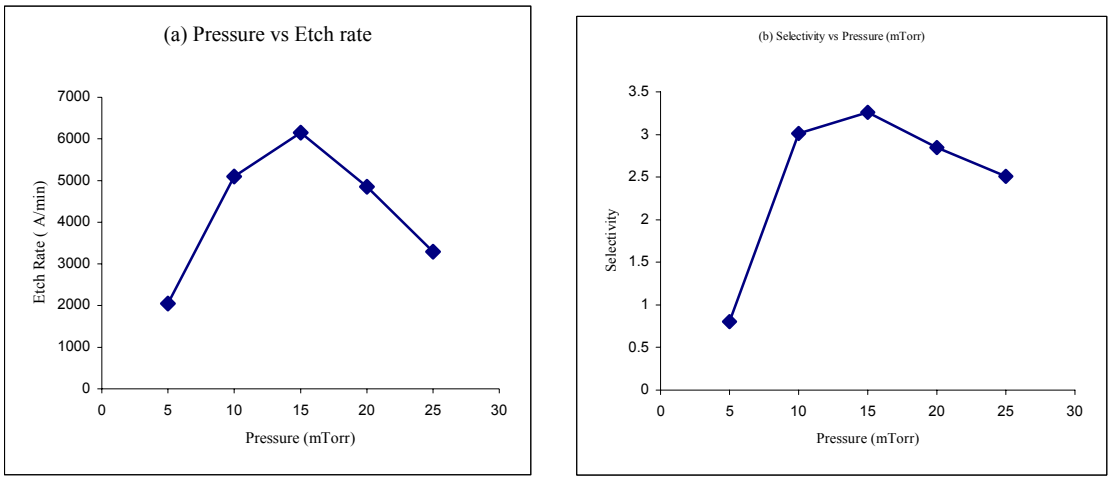

Figure 4. (a) Variations of p-AlGaN etch rates with different pressure (the ICP power is 600 W and chuck power 75 W); (b) plot of selectivity as a function of pressure.

The chlorine-etched samples were studied with a SEM for surface smoothness, and the SEM pictures are provided in figure 5 (a) and (b).

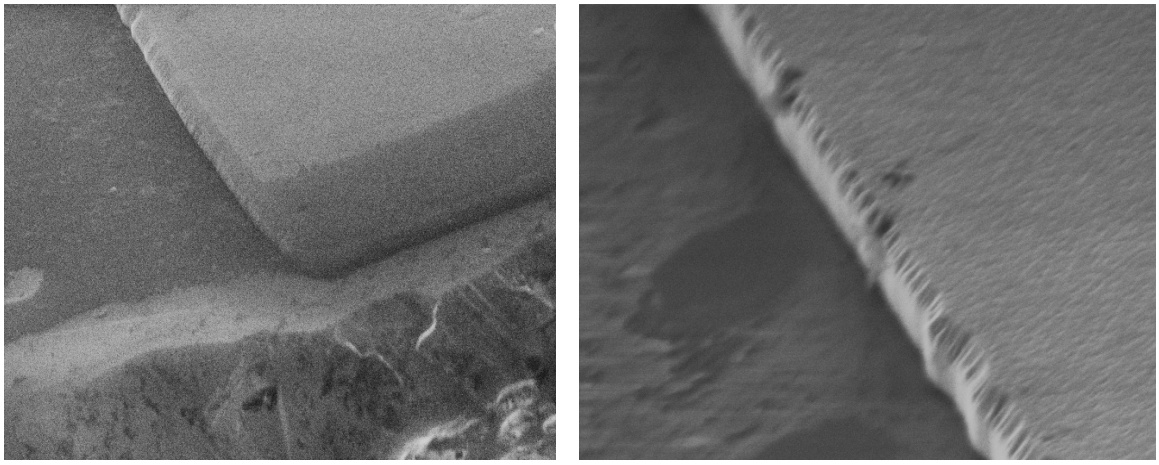

Figure 5. (a) Scanning electron micrographs of mesas etched at 20% Cl_2 in BCl_3/Cl_2; (b) SEM of 70 %Cl_2 in BCl_3/Cl_2 with ICP power of 600 W and chuck power 200 W.

At a lower concentration of chlorine, the damage is minimal and side walls are clearly defined with smooth anisotropy. However, at higher Cl_2 percentage, the damage on the side wall is obvious and there is visible side wall erosion which indicates that the Cl_2 component dominates the etching process by chemical reaction.

The surface morphology of etched p-AlGaN was examined with tapping AFM. The etched samples were scanned by this technique and representative images are shown in figure 6.

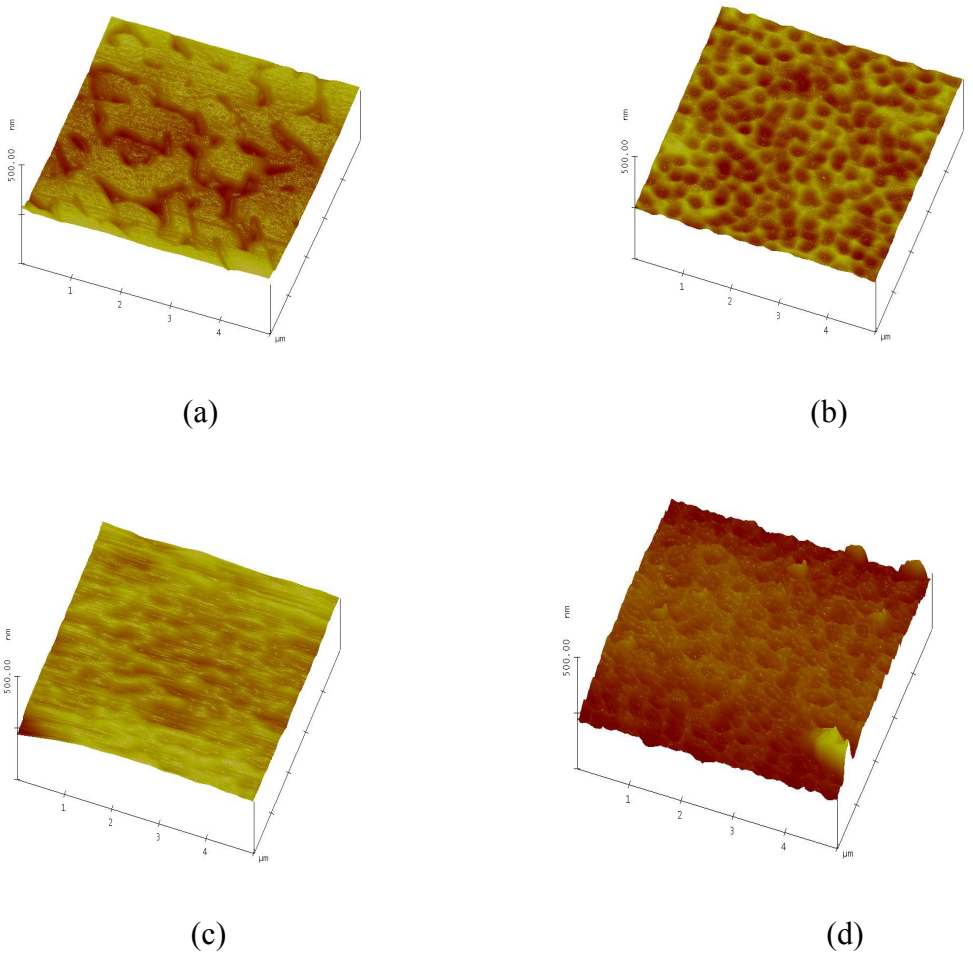

Figure 6. (a) AFM representative images of p-AlGaN ICP etched during various conditions: (a) an unetched control sample; (b) etched under chuck power change; (c) etched with percentage variations of Cl_2 in BCl_3/Cl_2; (d) etched under pressure change.

The surface roughness and the images change, depending on the way the samples were etched. The sampled area in all cases was 5 μm by 5 μm. The smoother etched surface in 6(c) appears to be related to the more stoichiometric removal of surface residue during the Cl_2 etching. The root mean square (rms) roughness was measured with the AFM, and the results are plotted in figure 7 for two cases.

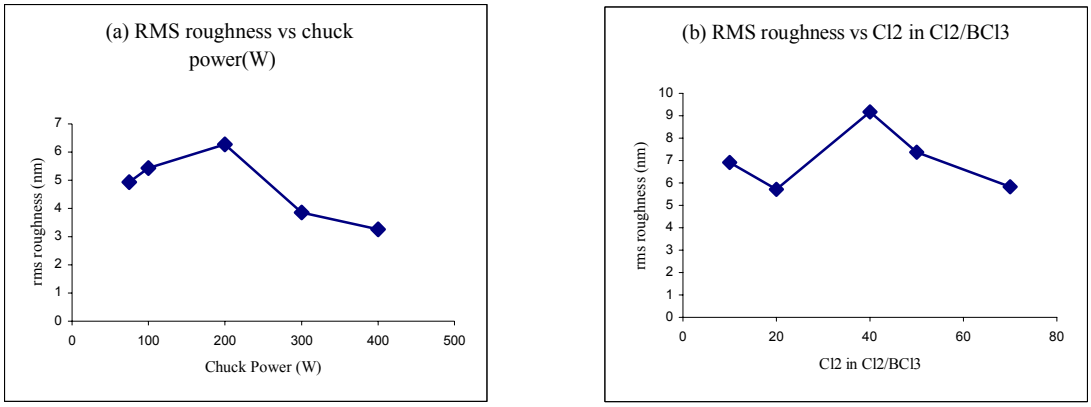

Figure 7. (a) RMS roughness values of p-AlGaN ICP etched samples (a) under various chuck power and (b) etched with percentage variations of Cl_2 in BCl_3/Cl_2.

In the case of roughness measurements with variations in chuck power, the rms roughness increases first, followed by a drop in the roughness, which indicates the smoothness of the surface because of high chuck power. The rough sharp features are removed faster than flat features, thus providing a smooth surface. In the second case of percentage variations of Cl_2 in BCl_3/Cl_2, the roughness increases as more and more chorine is added. However, the uniformity of roughness improves at a higher amount of chlorine.

A surface study was also performed on a number of etched and a control samples with AES analysis with a scan voltage of 3 kV. Results are shown in figure 8. The main change is the reduction of both Ga and N_2 signals in the etched sample. Calculations indicate that the Ga/N decreases by about 10%, which indicates a Ga deficiency in the etched surface.

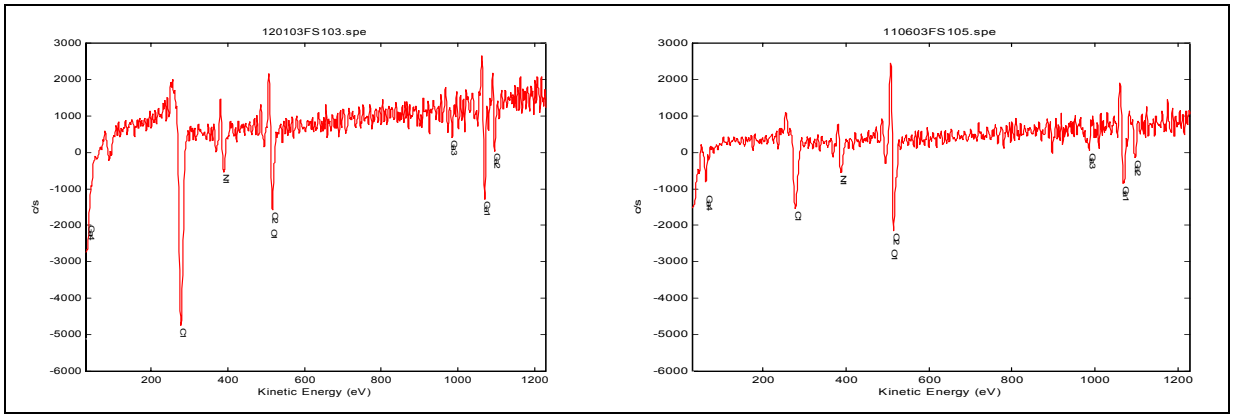

Figure 8. AES surface scan of (a) control sample p-AlGaN (b) etched sample. (The process conditions are 500 W of ICP power, 300 W chuck power, 20 sccm Cl_2, and 15 sccm BCl_3.)

4. Conclusion

In this study, we investigated MBE grown Mg-doped p-AlGaN etched by inductively coupled plasma with Cl_2/BCl_3 as etching gases. A detailed study of the samples was conducted and reported here with variations in chuck power, ICP power, Cl_2 ratio in Cl_2/BCl_3, and process pressure with a VLR series modular cluster plasma ICP processing system. From the study etching rates, selectivity, surface roughness, bearing analysis, SEM, and AES surface analysis were performed. It was found that p-AlGaN could be successfully etched by Cl_2/BCl_3 gas system. Etching rates were greatly enhanced by the rf chuck power, ICP source power, the chlorine concentration, and process pressure. The highest etching rates with ICP power change were about 5000 Å/min. The etching rate changed about 12% as the ICP power increased from 300 to 700 W. The selectivity improved three-fold. In using different RF chuck power, we found that the etching rate was more than doubled when the power increased from 75 W to 400 W of rf chuck power. The selectivity with respect to the photoresistance improved as the power increased. When changing the Cl_2 percentage in BCl_3/Cl_2 gas mixture to obtain etching rates, we found that the etching rates monotonically increased with the increase of chlorine and the selectivity showed marginal improvement initially but improved substantially to five-fold after 40% of chlorine was added to the BCl_3/Cl_2 gas mixture. In varying the pressure to change the etching rate, we found that the etching rate (even though initially increased at higher pressure) decreased. This decrease in etching rates can be explained as attributable to the mean free path changes that ions travel; the distance is much shorter at higher pressure than at 15 mTorr. At higher pressure, the KE is lower, creating more collisions between ions, causing the plasma to be much denser. The selectivity of p-AlGaN with respect to the photoresistance also shows a similar pattern. To find the surface morphology of etched samples, especially the ones etched by various percentages of chlorine, we observed that the damage on the etched samples at a lower concentration of chlorine is lower but at higher concentration, there is visible side wall erosion which indicated that the Cl_2 component dominates the etching process by chemical reaction.

The surface morphology of etched p-AlGaN samples was examined by AFM. It was found that the surface images changed depending on the way the samples were etched. Smoother etching surface was obtained with chlorine etching because of the stoichiometric removal of surface residue in this type of etching. The rms roughness increased first, followed by a drop in the roughness. This indicates the smoothness of the surface because of high chuck power and the rough sharp features were removed faster than the flat features, thus providing a smooth surface. This report documents for the first time the bearing analysis of MBE grown Mg-doped p-AlGaN samples. Bearing analysis indicated that the control sample had a larger bearing area, meaning that it has a larger surface area above or below a given height whereas for the chlorine etched and other etched samples, these values were lower, indicating that the etched samples are smoother. However, the etched samples had larger areas of uneven surface compared to the

control sample, as shown the histogram. AES studies of the control and etched samples indicate the reduction of Ga and N_2 signals in the etched sample. Calculations indicate that Ga/N decreases by 10% in the etched sample, indicating a Ga deficiency in the etched sample.

5. References

1. Nakamura, S. *IEEE J. Sel. Top, Quantum Electron* **1998**, *4*, 483.
2. Nakamura, S.; Fasol, G. *The Blue Laser Diode* (Springer, Berlin. 1997)
3. Ren, F.; Abernathy, C. R.; Van Hove, J. M.; Chow, P. P.; Hickman, R.; Klassen, J. J.; Kopf, R. F.; Cho, H.; Jung, K. B.; La Roche, J. R.; Wilson, R. G.; Han, J.; Shul, R. J.; Baca, A. G.; Pearton, S. J. *MRS Jnl. Internet Semicond. Res.* **1998**, *3*, 41.
4. McCarthy, L. S.; Kozodoy, P.; Den Baaars, S. P.; Rodwell, M.; Mishra, U. K. *25th Intl. Symp. Comp. Semicond.*, Nara. Japan. October 1998.
5. Han, J.; Baca, A. G.; Shul, R .J.; Willison, C.; Zhang, G. L.; Ren, F.; Zhang, A. P.; Dang, G. T.; Donovan, S. M.; Cao, X. A.; Cho, H.; Jung, K. B.; Abernathy, C. R.; Pearton, S. J.; Wilson., R. G. *Appl. Phys Lett.* **1999**, *74*, 2702.
6. Osinsky, A.; Gangopadhyay, S.; Gaska, R.; Williams, B.; Khan, M. A.; Kuksenkov, D.; Temkin, H. *Appl. Phys. Lett.* **1997**, *71*, 2334.
7. Van Hove, J. M.; Hickman, R.; Klassen, J. J.; Chow, P. P.; Ruden, P. D. *Appl. Phys. Lett.* **1997**, *70*, 2282.
8. Yang, W.; Nohava, T.; Krishnankutty, S.; Toucaro, R.; Mcpherson, S.; Marsh, H. *Appl. Phys. Lett.* **1998**, *73*, 1086.
9. Zhang, L.; Lester, L. F.; Baca, A. G.; Shul, R. J.; Chang, P. C.; Willison, C. G.; Mishra, U. K.; Denbaars, S. P.; Zolper, J. C. *IEEE Trans. Electron Devices* **2000**, *47*, 507.
10. Wraback, M.; Shen, H.; Carrano, J. C.; Collins, C. J.; Campbell, J. C.; Dupuis, R. D.; Shurman, M. J.; Ferguson, I. T. *Appl. Phys. Lett.* **2001**, *79*, 1303.
11. Shul, R. J.; Zhang, L.; Baca, A. G.; Willison, C. G.; Han, H.; Pearton, S. J.; Ren, F. J. *Vac. Sci. Technol* **2000**, *A 18*, 1139.
12. Pearton, S. J.; Abernathy, C. R.; Ren, F. *Appl.Phys Lett.* **1994**, *64*, 2294.
13. Vartuli, C. B.; Pearton, S. J.; Lee, J. W.; Hong, J.; Mckenzie, J. D.; Abernathy, C. R.; Shul, R. J. *Appl. Phys Lett.* **1996**, *69*, 1426.
14. Shul, R. J.; McClellan, G. B.; Casalnuova, S. A.; Rieger, D. J.; Pearton, S. J.; Constantine, C.; Barr, C.; Karlick, R. F. Jr.; Tran, C.; Schurman, M. *Appl. Phys Lett.* **1996**, *69*, 1119.

15. Shul, R. J.; Zhang, L.; Baca, A. G.; Willison, C. G.; Han, J.; Pearton, S. J.; Hong, J.; Abernathy, C. R.; Lester, L. F. *MRS. Internet J. Nitride Semiconductors, Res. 4S1.G8.1* 1999.

16. Smith, S. A.; Wolden, C. A.; Bremser, M. D.; Hanser, A. D.; Davis, R.. F.; Lampert, W. V. *Appl. Phys Lett.* **1997**, *71*, 3631.

17. Khan, F. A.; Zhou, L.; Ping, A. T.; Adesida, I. *J. Vac. Sci. Technol* **1999**, *B 17*, 2750.

18. Hahn, Y. B.; Im, Y. H.; Park, J. S.; Nahm, K. S.; Lee, Y. S. *J.Vac. Sci. Technol* **2001**, *A 9*, 1277.

19. Tripathy, S.; Ramam, A.; Chua, S. J.; Pan, J. S.; Huan, Alfred *J.Vac. Sci. Technol* **2001**, *A 19*, 2522.

20. Im, Y. H.; Park, J. S.; Hahn, Y. B.; Nahm, K. S.; Lee, Y-.S.; Cho, B. C.; Lim, K. Y.; Lee, H. J.; Pearton, S. J. *J. Vac. Sci. Technol* **2000**, *A 18*, 2169.

21. Van Hove, J. M.; Cosmini, G. J.; Nelson, E.; Wowchak, A. M.; Chow, P. P. *J. Cryst. Growth* **1995**, *150*, 908.

Distribution List

ADMNSTR
DEFNS TECHL INFO CTR
ATTN DTIC-OCP (ELECTRONIC COPY)
8725 JOHN J KINGMAN RD STE 0944
FT BELVOIR VA 22060-6218

DARPA
ATTN IXO S WELBY
3701 N FAIRFAX DR
ARLINGTON VA 22203-1714

OFC OF THE SECY OF DEFNS
ATTN ODDRE (R&AT)
THE PENTAGON
WASHINGTON DC 20301-3080

US ARMY TRADOC
BATTLE LAB INTEGRATION & TECHL DIRCTRT
ATTN ATCD-B
10 WHISTLER LANE
FT MONROE VA 23651-5850

US MILITARY ACDMY
MATHEMATICAL SCI CTR OF EXCELLENCE
ATTN LTC T RUGENSTEIN
THAYER HALL RM 226C
WEST POINT NY 10996-1786

SMC/GPA
2420 VELA WAY STE 1866
EL SEGUNDO CA 90245-4659

US ARMY ARDEC
ATTN AMSTA-AR-TD
BLDG 1
PICATINNY ARSENAL NJ 07806-5000

COMMANDING GENERAL
US ARMY AVN & MIS CMND
ATTN AMSAM-RD W C MCCORKLE
REDSTONE ARSENAL AL 35898-5000

US ARMY INFO SYS ENGRG CMND
ATTN AMSEL-IE-TD F JENIA
FT HUACHUCA AZ 85613-5300

US ARMY NATICK RDEC
ACTING TECHL DIR
ATTN SBCN-TP P BRANDLER
KANSAS STREET BLDG 78
NATICK MA 01760-5056

US ARMY SIMULATION TRAIN & INSTRMNTN CMND
ATTN AMSTI-CG M MACEDONIA
12350 RESEARCH PARKWAY
ORLANDO FL 32826-3726

AIR FORCE RESEARCH LAB
MATERIALS DIRECTORATE
ATTN W V LAMBERT
WRIGHT PATTERSON AFB OH 45433

SANDIA NATL LAB
ATTN R J SHUL
ALBUQUERQUE NM 87185

KWANGJU INSTITUTE OF SCIENCE AND TECH
DEPT OF MATERIAL SCIENCE AND ENG
CENTER FOR OPTOELECTRONIC MATERIAL RESEARCH
ATTN SEONG-JU PARK
KWANGJU 500-712 KOREA

UNIVERSITY OF ILLINOIS
MICROELECTRONICS LAB
DEPT OF ELECTRICAL AND COMPUTER ENG
ATTN PROF ADESIDA
URBANA IL 61801

UNIVERSITY OF CALIFORNIA
DEPT OF ELECTRICAL AND COMPUTER ENG
ATTN U K MISHRA
SANTA BARBARA CA 93106

TUSKEGEE UNIVERSITY
DEPT OF ELECTRICAL ENG
ATTN K DAS
TUSKEGEE AL 36088

UNIVERSITY OF NEW MEXICO
DEPT OF ELECTRICAL ENG
ATTN L F LESTER
ALBUQUERQUE NM 87131

NORTH CAROLINA STATE UNIVERSITY
DEPT OF MATERIAL SCIENCE AND ENG
ATTN R F DAVIS
RALEIGH NC 27695

UNIVERSITY OF FLORIDA
DEPT OF MATERIAL SCIENCE AND ENG
ATTN C R ABERNATHY
GAINESVILLE FL 32611

UNIVERSITY OF FLORIDA
DEPT OF MATERIAL SCIENCE AND ENG
ATTN S J PEARTON
PO BOX 116400
GAINESVILLE FL 32611

CHONBUK NATIONAL UNIVERSITY
SCHOOL OF CHEMICAL ENG AND TECH
SEMICONDUCTOR PHYSICS RESEARCH CTR
ATTN Y B HAHN
CHONJU 561-756 KOREA

A DABIRAN
7620 EXECUTIVE DR
EDEN PRAIRIE MN 55344

NATIONAL UNIVERSITY OF SINGAPORE
CENTER OF OPTOELECTRONICS
DEPT OF ELECTRICAL AND COMPUTER ENG
ATTN S TRIPATHY
SINGAPORE 119260

HICKS & ASSOC INC
ATTN G SINGLEY III
1710 GOODRICH DR STE 1300
MCLEAN VA 22102

INSTITUTE OF MATERIAL RESEARCH AND ENG
ATTN A RAMAM
3 RESEARCH LINK
SINGAPORE 117602

PALISADES INST FOR RSRCH SVC INC
ATTN E CARR
1745 JEFFERSON DAVIS HWY STE 500
ARLINGTON VA 22202-3402

SVT ASSOCIATES
ATTN J M VAN HOVE
EDEN PRAIRIE MN 55344

UNAXIS, INC
ATTN C BARRAT
ATTN C CONSTANTINE
ST PETERSBUGH FL 33716

DIRECTOR
US ARMY RSRCH LAB
ATTN AMSRD-ARL-RO-D JCI CHANG
ATTN AMSRD-ARL-RO-EN W D BACH
PO BOX 12211
RESEARCH TRIANGLE PARK NC 27709

US ARMY RSRCH LAB
ATTN AMSRD-ARL-D J M MILLER
ATTN AMSRD-ARL-CI-OK-T TECHL PUB (2 COPIES)
ATTN AMSRD-ARL-CI-OK-TL TECHL LIB (2 COPIES)

ATTN IMNE-AD-IM-DR MAIL &
RECORDS MGMT
ATTN AMSRD-ARL-SE
ATTN AMSRD-ARL-SE-D
ATTN AMSRD-ARL-SE-DC
ATTN AMSRD-ARL-SE-DE
ATTN AMSRD-ARL-SE-DP
ATTN AMSRD-ARL-SE-DS
ATTN AMSRD-ARL-SE-E
ATTN AMSRD-ARL-SE-EE
ATTN AMSRD-ARL-SE-EI
ATTN AMSRD-ARL-SE-EI P BOYD
ATTN AMSRD-ARL-SE-EI U LEE
ATTN AMSRD-ARL-SE-EM
ATTN AMSRD-ARL-SE-EM
F SEMENDY
ATTN AMSRD-ARL-SE-EO
ATTN AMSRD-ARL-SE-L
ATTN AMSRD-ARL-SE-R
ATTN AMSRD-ARL-SE-RE
ATTN AMSRD-ARL-SE-RL
ATTN AMSRD-ARL-SE-RM
ATTN AMSRD-ARL-SE-RU
ATTN AMSRD-ARL-SE-S
ATTN AMSRD-ARL-SE-SA
ATTN AMSRD-ARL-SE-SE
ATTN AMSRD-ARL-SE-SG
ATTN AMSRD-ARL-SE-SH
ATTN AMSRD-ARL-SE-SS
ADELPHI MD 20783-1197